Available online at www.sciencedirect.com
SCIENCE DIRECT
Catalysis Today 110 (2005) 140–153
CATALYSIS TODAY
www.elsevier.com/locate/cattod

Selective oxidation of carbon monoxide in a hydrogen-rich fuel cell feed using a catalyst coated microstructured reactor

V. Cominos [a,*], V. Hessel [a], C. Hofmann [a], G. Kolb [a], R. Zapf [a], A. Ziogas [a], E.R. Delsman [b], J.C. Schouten [b]

[a] *Institut für Mikrotechnik Mainz GmbH, Carl-Zeiss-Str. 18-20, 55129 Mainz, Germany*
[b] *Eindhoven University of Technology, P.O. Box 513, 5600 MB Eindhoven, The Netherlands*

Available online 11 October 2005

Abstract

Carbon monoxide is known to be poisonous to the proton exchange membrane fuel cell catalyst. Selective oxidation of carbon monoxide in a hydrogen-rich reformate stream is considered to be a practical method with the most potential for reducing concentrations down to tolerant levels. In the present work, nine different noble metal catalysts were investigated using a microstructured reactor in the presence of excess hydrogen and carbon dioxide at a GHSV of 15 500 h^{-1} and at temperatures up to 160 °C. The most active were Pt–Ru/γ-Al_2O_3, Rh/γ-Al_2O_3 and Pt–Rh/γ-Al_2O_3 yet the most stable was Pt–Rh/γ-Al_2O_3. Its activity was also investigated using a wet feed and also at a GHSV of 31 000 h^{-1}. Water was found to promote the catalyst activity while at higher GHSV higher temperatures were required to achieve full carbon monoxide conversion. The catalyst exhibited steady performance in the microstructured reactor for 50 h while reducing 1.12% carbon monoxide to 10 ppm with inlet oxygen to carbon monoxide ratio of 4.

Keywords: Carbon monoxide; Selective oxidation; Fuel cell; Microstructured reactor

1. Introduction

To-date, proton exchange membrane (PEM) fuel cells continue to be extensively studied as they promise to deliver cleaner energy at a higher efficiency. With the exception of direct methanol fuel cells, pure H_2 is considered to be the best fuel for operating proton exchange membrane fuel cells yet obstacles such as size, weight, cost and technical limitations still remain regarding the storage of H_2 [1]. Fuel reforming is an alternative method for providing H_2 on demand but requires CO clean-up stages such as water–gas-shift reactors (with the exception of methanol reforming systems) followed by either pressure swing adsorption, methanation or selective oxidation as even trace amounts of CO can poison the fuel cell catalyst. CO removal by pressure swing adsorption requires expensive compressors while methanation becomes more complex due to the hydrogenation of CO_2 which is also present in reformate streams. Since selective oxidation of CO takes place at low temperatures, under atmospheric pressure and is relatively inexpensive it is considered to be a practical method with the most potential.

Efforts in developing catalysts and entire selective oxidation reactors are continuing as it is necessary that the catalyst used functions within the temperature region defined by the energy balance of the overall fuel processing system, exhibits high CO oxidation selectivity as opposed to the undesired H_2 oxidation, is resistant to deactivation in the presence of CO_2 and H_2O, and in addition possesses high CO oxidation activity [2].

CO levels need to be decreased to at least below 50 ppm as dictated by the poisoning limit of a Pt fuel cell catalyst [1]. Levels in a stream leaving a water–gas-shift reactor typically lie between 0.5 and 2 vol.% and not significantly more than 1 vol.% in a stream directly leaving a methanol reformer.

CO oxidation is a well-studied reaction yet the selective oxidation of CO in the presence of H_2, CO_2 and H_2O has not been studied to the same extent even though a connection exists due to the water–gas-shift reaction [3–5]. Pt/Al_2O_3 has been extensively studied as a selective CO oxidation catalyst [3,6–8]. Promoted Pt/Al_2O_3 catalysts have also been investigated [9–11]. Performances of other noble metals such as Ru, Rh and Pd

* Corresponding author.
E-mail address: vania_cominos@yahoo.co.uk (V. Cominos).

0920-5861/$ – see front matter © 2005 Elsevier B.V. All rights reserved.
doi:10.1016/j.cattod.2005.09.008

have additionally been investigated [12,13]. It is difficult, though, to compare studies carried out by various research teams as reaction conditions differ. Review papers such as that of Trimm and Önsan [14] and that of Ghenciu [1] report on the various fuel processing catalysts, including those for the selective oxidation of CO, investigated by various teams. There are few papers though which specifically report decrease of CO concentrations down to ppm levels [11,13,15,16] and an even more limited number of studies exist on selective oxidation of CO in compact or microstructured reactors [15–18].

Bringing CO levels to below 50 ppm does not only require an active catalyst but also good reactor design. A key issue for efficient reactor operation in terms of reducing CO to levels acceptable for PEM fuel cells is that of thermal management. Thus, a compact device is preferable in order to achieve high surface area-to-volume ratio and high heat and mass transfer efficiency [19]. Microchannels are known to achieve these properties in addition to lower pressure drops as compared to packed catalyst beds. Most importantly, they are suitable for washcoating and thus improved catalyst utilisation can be achieved through the enhanced mass and heat transfer rates offered.

Dudfield et al. [15] presented a 20 kW compact aluminium plate-fin heat exchanger-selective oxidation reactor system incorporating a Pt–Ru/hopcalite catalyst. The dual-stage reactor system achieved a reduction of 2.7% CO down to less than 20 ppm in the presence of a complete reformate stream, with temperatures between 150 and 160 °C and using a total O_2/CO ratio of 3. This was a continuation of their work reported earlier [17,18].

Chen et al. [16] presented a microstructured reactor, which incorporated a Rh–K/Al_2O_3 catalyst. In the presence of a complete reformate stream, at a temperature of 187 °C, GHSV of 20 000 h^{-1} and using an O_2/CO ratio of 1.5, they reduced 0.5% CO to 20 ppm.

Work presented in the current paper was carried out within the framework of the European project "Micro Reactor Technology for Hydrogen and Electricity" (acronym MiRTH-e; contract no. EN6K-CT-2000-00110). Part of the overall project aim was to design, fabricate and test a microstructured reactor

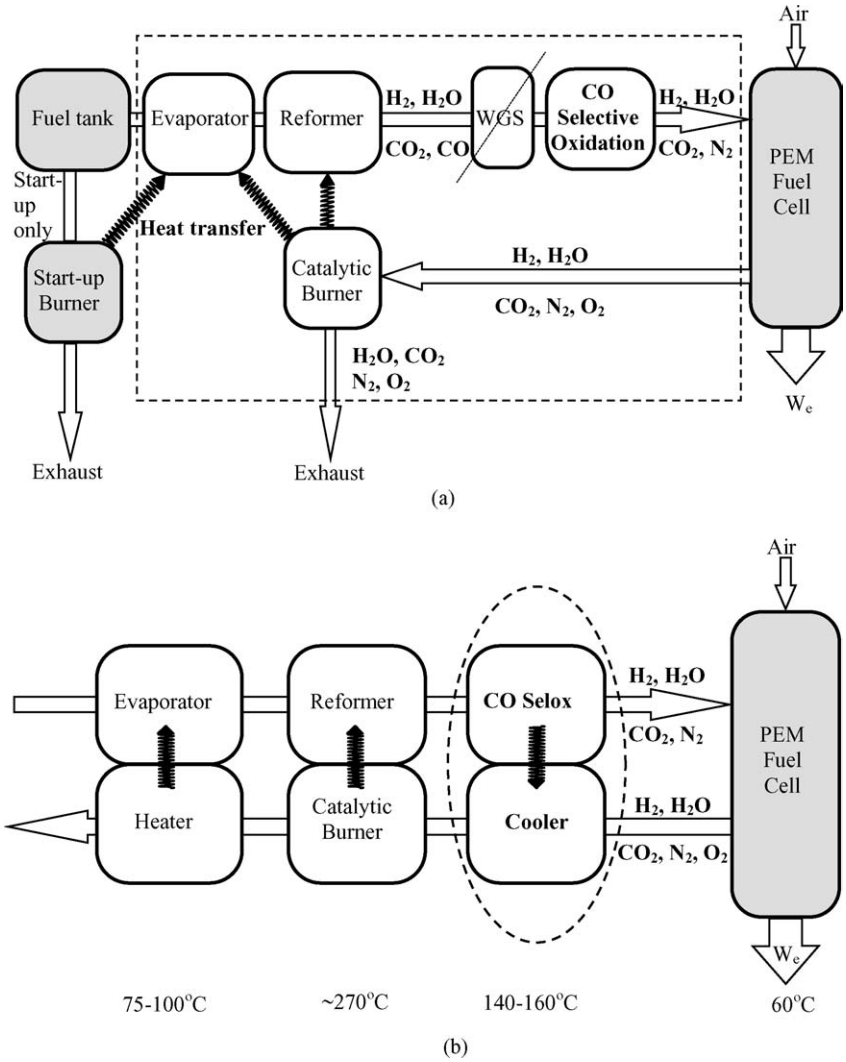

Fig. 1. (a) Devices typically present in a fuel processor for PEM fuel cells. (b) The basic layout of the MiRTH-e fuel processing system and the operating temperatures of devices.

for the selective oxidation of CO to be used in a 100 W methanol fuel processor. Work on this project has been previously reported by Delsman et al. [20,21]. In the current paper, the work regarding the investigation of nine different catalyst washcoats applied within the MiRTH-e first generation integrated selective oxidation-heat exchanger microstructured reactor and the overall performance of the opted final catalyst is presented.

2. Reactor design

A typical fuel processing system for a PEM fuel cell (a schematic layout is shown in Fig. 1a) consists of a number of units namely, a fuel tank, a start-up burner, an evaporator (if the fuel is a liquid), a reformer, a water–gas-shift reactor, a selective oxidation reactor and a catalytic burner. If the fuel reformed is methanol then a water–gas-shift reactor is not required as CO levels in the reformer exit stream do not considerably exceed 1% as was the case in the MiRTH-e project. Thus, the CO clean-up is carried out in a selective oxidation reactor alone in order to bring levels down to well below 50 ppm to ensure efficient operation of a PEM fuel cell.

To balance the heat produced and the heat required by the various units incorporated in a methanol steam reforming system, devices may be coupled as shown in Fig. 1b. Thus, the water methanol mixture entering the evaporator may be heated by a coupled heater (to 75–100 °C) while the hot reformate stream leaving the coupled reformer-burner device (at ca. 270 °C) may be cooled to CO oxidation temperatures (ca. 140–160 °C) by the cooler stream leaving the PEM fuel cell (at ca. 60 °C) consisting of the unutilised H_2. This may be burnt catalytically to provide energy to a coupled steam reformer. The hot exit stream of the burner may then further provide energy to the methanol evaporator. Thus, the MiRTH-e selective CO oxidation microstructured reactor prototype was designed to function as a counter-current heat exchanger as indicated by its flow path shown in Fig. 2.

The reason for integrating the top heat exchanger to the reactor part is such that the temperature of the reformate stream can be brought down to the temperature of ca. 150 °C (from ca. 270 °C) for the catalytic selective oxidation of the CO to take place. The stream should then be further cooled down by the bottom heat exchanger to a temperature of ca. 65 °C which is low enough for it to enter a low temperature PEM fuel cell. The cooling stream is a combined anode and cathode exhaust leaving the fuel cell (see Fig. 1a) and consists, among other compounds, of the unutilised H_2 (ca. 5%). This stream is heated up as it passes through the heat exchangers, in a counter-current fashion to the reformate stream, and should exit the device at a temperature high enough for the H_2 to be combusted in the catalytic burner (ca. 200 °C) in order to provide sufficient energy for the endothermic reforming reaction taking place in the coupled reformer reactor. The three sections, namely the high and low temperature heat exchangers (one at the top and the other at the bottom of the device) and the selective oxidation reactor-heat exchanger (in the middle of the device), are shown in Fig. 2. The three heat exchanging sections are

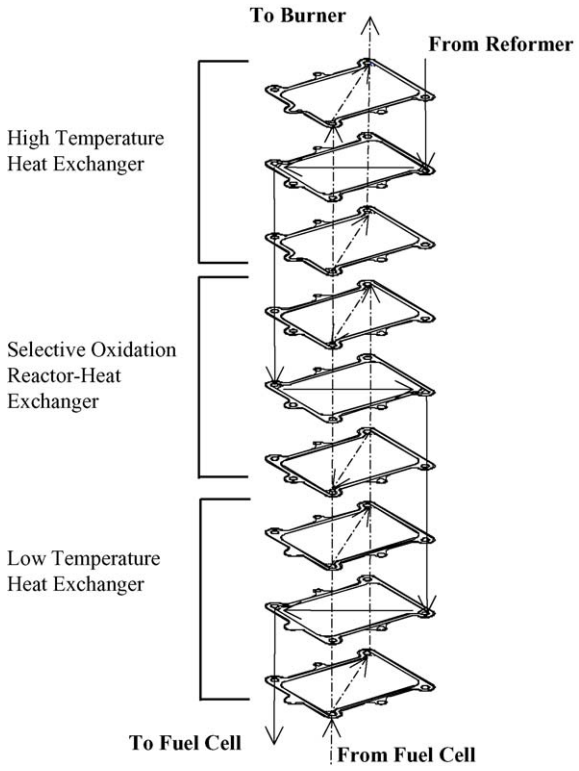

Fig. 2. Flow path within the microstructured reactor.

thermally separated from each other and from the top and bottom housing parts by 4 mm thick Klingersil® plates (not shown in figure).

The overall microstructured reactor (shown in Fig. 3) has dimensions of 50 mm × 53 mm × 66 mm and consists of 0.5 mm thick stainless steel plates with etched microchannels and laser machined outer contours. Graphite seals are incorporated to achieve leak tightness and flexibility in exchanging catalytically coated plates. The selective oxidation reactor-heat exchanger core part of the device incorporates 19 plates each with 82 catalytically coated microchannels with dimensions 0.25 mm × 0.187 mm × 30 mm. The 10 plates through which the cool stream from the fuel cell flows

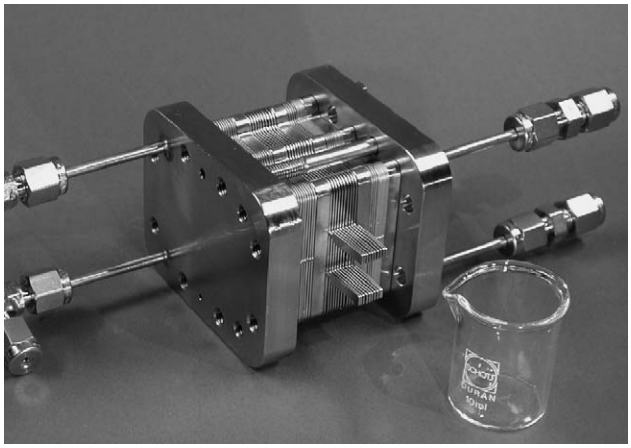

Fig. 3. Microstructured integrated selective oxidation reactor-heat exchanger prototype.

have 75 microchannels with dimensions of 0.25 mm × 0.125 mm × 30 mm. Both the high temperature heat exchanger and the low temperature heat exchanger incorporate two plates on the hot reformate stream side and four plates on the coolant stream side. Each plate consists of 58 channels with dimensions of 0.4 mm × 0.3 mm × 30 mm. More detailed description of the device has been reported by Delsman et al. [20].

The aim was to have a flexible device where the catalytically coated plates could be exchanged while at the same time the temperature of the reformate stream could be brought down to the temperature of approximately 150 °C (from approximately 270 °C) for catalytic selective oxidation of the CO to take place. During the experiments, a N_2 stream was used instead of a fuel cell exhaust stream.

3. Catalyst preparation and characterisation

The catalysts presented in this paper were prepared as washcoats and tested by IMM. The coating of the plates with home-made catalysts was carried out by first applying manually a γ-alumina or an α-alumina washcoat onto the entire length of the etched stainless steel channels. A 20% alumina suspension was prepared from γ-alumina or α-alumina (both purchased from Alfa Aesar) and deionised H_2O. The suspensions also consisted of 5% polyvinyl alcohol binder (purchased from Fluka) and 1% acetic acid. The channels were then filled with the relative suspension and any excess on the top of the channel walls was wiped off. The washcoated plates were then calcined for 2 h at a temperature of 600 °C. Prior to impregnation, plates were placed in vacuum to remove air from the pores and CO_2 was then passed to fill the pores. Incipient wetness impregnation was then performed with aqueous solutions of H_2PtCl_6 (99.9% purity, purchased from ABCR), $Co(NO_3)_2$ (99% purity, purchased from Fluka), $RhCl_3$ (purchased from ABCR) or mixtures depending on the catalyst wished to be prepared.

The procedure for applying commercial powder catalysts (purchased from Degussa) as washcoats was similar to that of applying a washcoat for home-made catalysts with the exception being that there was no impregnation step as the active metal was already present in the washcoat. Five percent Rh/γ-alumina (G213 KR/D Degussa), 5% Pt/γ-alumina (F214 VH/D Degussa) and 10% Ru/γ-alumina (H213 KR/D Degussa) were the commercial catalysts used. For bimetallic catalysts, either a commercial Pt/γ-alumina catalyst was mixed together with a commercial Rh/γ-alumina catalyst to form one washcoat or a commercial catalyst such as Rh/γ-alumina was mixed together with ceria (method A). For preparing the combined home-made with commercial catalyst, a commercial Pt/γ-alumina catalyst was first applied as a washcoat onto the channels and then a $RhCl_3$ precursor was used to impregnate the Rh into the washcoat (method B). The average thickness of each washcoat was ca. 40 μm in channels with widths of 250 μm and depths of 187 μm.

After calcinations at 600 °C, the catalyst coated plates were incorporated into the microstructured reactor and were mildly reduced under a flow of 55% H_2 in N_2 at 500 ml/min (STP) while initially being heated at a ramp rate of 3 °C/min from room temperature to 130 °C and then for one hour at this constant temperature. The reactor was then purged with N_2 while cooling down. Mild reduction conditions were chosen in order to avoid further loss of OH groups due to high temperatures as these groups are expected to play a role in the activity of the catalysts [22].

The physical properties of the catalysts prepared are shown in Table 1. The catalysts names are given based on their metal state (and will be referred as such throughout the paper) even though this may not be their real state due to the pre-treatment conditions. The surface area and maximum pore diameter of the fresh catalysts were determined through BET measurements (N_2 adsorption) while a few H_2 chemisorption measurements were made to qualitatively determine the differences in mean particle sizes of the mildly reduced catalysts. For bimetallic catalysts the value found was an average for the mildly reduced Pt and Rh species.

Fig. 4 shows the temperature programmed reduction (TPR) profiles of fresh catalysts after calcination and mild reduction pre-treatment steps have been carried out. It should be noted that the mass of the individual samples varied and thus the intensity of the peaks was affected. Starting from the profile of

Table 1
Physical properties of fresh catalysts

Catalyst	Overall loading (wt.%)	Max. pore diameter (nm)	BET specific surface area (m^2/g)	Overall catalyst mass (mg)	Mean particle diameter (nm)
Pt/γ-Al_2O_3[a]	5	4	217	250	12
Rh/γ-Al_2O_3[a]	5	6	134	250	1.8
Ru/γ-Al_2O_3[a]	10	5	60	150	–
Ru/CeO_2/γ-Al_2O_3	5	20	58	250	–
Rh/CeO_2/γ-Al_2O_3	5	8	50	250	–
Pt–Ru/γ-Al_2O_3 (1Pt:1Ru)	5	4	182	250	–
Pt–Co/γ-Al_2O_3 (1Pt:1Co)	5	14	65	250	–
Pt–Rh/γ-Al_2O_3[b] (1Pt:1Rh)	10	5	238	250	1.4 (Pt + Rh)
Pt–Rh/γ-Al_2O_3[c] (1Pt:1Rh)	5	9	161	250	1.0 (Pt + Rh)
Pt–Rh/α-Al_2O_3 (1Pt:1Rh)	5	37	11	250	–

[a] Degussa catalysts.
[b] Prepared by method B.
[c] Prepared by method A.

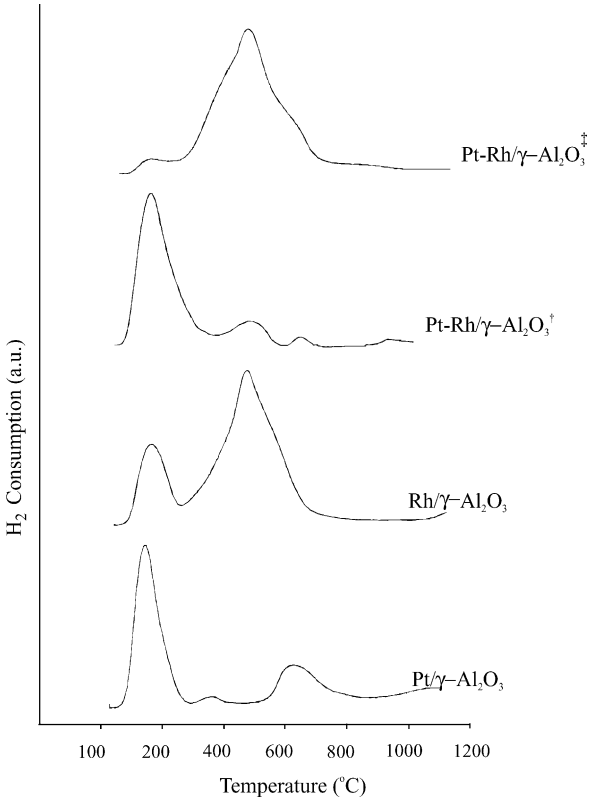

Fig. 4. TPR profiles of Pt/γ-Al_2O_3, Rh/γ-Al_2O_3 and Pt–Rh/γ-Al_2O_3 catalysts; † prepared by method B; ‡ prepared by method A.

Pt/γ-alumina (sample mass was ca. 0.3 g) three different peaks may be seen corresponding to three different species present on the catalyst surface. The first and biggest peak appearing was at the low temperature of ca. 140 °C which may correspond to the Pt metal state. A much smaller peak appeared at 370 °C and a slightly bigger peak at 640 °C probably showing the presence of other oxide states of the metal catalyst. The Rh/γ-alumina catalyst (sample mass ca. 0.135 g) also exhibited a first peak at ca. 140 °C, but with a slightly different shape, most probably indicating Rh metal state. A much bigger peak was exhibited at the temperature of 470 °C. The Pt–Rh/γ-alumina catalyst washcoat (sample mass of ca. 0.2 g) prepared by method B exhibited the first peak typical for both Pt and Rh at ca. 140 °C and then a smaller peak at 470 °C typically belonging to Rh. A third peak appeared at the temperature of 640 °C typical of a Pt species. The Pt–Rh/γ-alumina catalyst washcoat (sample mass of ca. 0.07 g) prepared by method A exhibited a small peak at ca. 140 °C typical for both Pt and Rh but then a significantly larger peak at 470 °C which is typical only of Rh. The two different profiles of these last two catalysts may well lie in the differences in method of preparation used. Thus, from preparation method A it can be concluded that significantly more Rh species are found on the catalyst surface than Pt species, while with preparation method B a better mixture of Pt and Rh species are found on the catalyst surface, the dominant though possibly being that of Pt. The synergy of the metals in the two washcoats is therefore expected to be different.

The TPR profiles also indicate that the mild reduction pre-treatment of the catalysts does not bring them entirely to their metal state as the pre-treatment temperature is approximately 10 °C lower than the first peak exhibited by the three catalysts (namely, 140 °C). This may limit catalyst deactivation under reaction conditions, due to oxidation of the active catalyst species by the O_2 reactant, while OH groups still present due to the low temperatures applied may improve activity.

4. Experimental procedure

4.1. Reactor operation

The reactor was operated in an integral mode during catalyst performance experiments to examine the effects of temperature, O_2/CO ratio, H_2O, space velocity and catalyst preparation method on catalyst activity. The reaction temperature was considered to be the temperature detected at the gas exit side of the second heat-exchanging part (in which the catalyst coated plates were incorporated) by using a 0.5 mm thick thermocouple.

Tests were carried out with catalyst loadings as shown in Table 1, under atmospheric pressure and total flowrate of 550 ml/min (STP) which corresponds to a gas hourly space velocity (GHSV) of 15 500 h^{-1}. GHSV is here defined as the ratio of the volumetric flowrate of the feed stream at STP to the volume of the catalyst coated channels. The operating conditions used are similar to those of the overall fuel processor operating at half load. Experiments under full load conditions were only carried out to examine the effect of space velocity. The reason for not carrying out all experiments under full load conditions was simply in order not to consume large amounts of gases. In addition, as the present reactor design did not achieve a fast heating up time (due to the bulky top and bottom plates and the screws used for compressing the gaskets) a heating cable was used to speed up the heating time which would not normally be the case in a fuel processor.

Gas flows were regulated by Bronkhorst mass flow controllers. A special gas mixture consisting only of H_2, CO_2 and CO was purchased from Linde AG gas (class 1). The dry feed simulating the reformate stream was composed of 57% H_2, 21% CO_2, 1.12% CO, 4.48% O_2, balance N_2. The ratio of N_2 to O_2 at the feed was approximately that of air as would be the real case in a fuel processor. It was only varied when carrying out experiments with different O_2/CO ratios. For experiments with a wet feed, a Bronkhorst liquid flow controller and evaporator were used for feeding H_2O vapour. The wet feed was composed of 54% H_2, 19% CO_2, 0.94% CO, 3.76% O_2 10% H_2O, balance N_2. The ratio of N_2 to O_2 was in this case slightly below that of air. The small differences in the species concentrations as compared to the dry feed arise due to the fact H_2, CO_2 and CO were a fixed mixture coming from one gas cylinder and that the total flow rate was kept the same. The O_2/CO ratio was kept as 4 while the amount of N_2 present was slightly lower than what would be expected if air was used instead. These differences, though, are not considered to have any influence on the results. All feeds were heated before entering the microstructured device while pure N_2 was used in all cases to simulate the cooling stream coming from the fuel cell side. Product gases flowed through a heated line before

entering the gas chromatograph in order to avoid any water condensation from taking place.

4.2. Gas analysis

The concentration of the various species present in the reactor off-gas was detected by an online gas chromatograph (Varian CP-4900 Micro-GC). It consisted of four different channels each with a separate TCD detector and oven. Channel 1 had a 10 m long Molsieve column which could separate O_2, N_2 and CO, channel 2 had a similar column to separate H_2 and CH_4, channel 3 had a Porapak U column to separate CO_2, H_2O and species up to butane. Channel 4 was not used in this work as it had a column for separating alkanes above butane. All channels used helium as carrier gas with the exception of channel 2 which used N_2 as carrier gas and column pressure was in all cases 150 kPa. Each analysis lasted for 1 min while it was possible to have an analysis cycle of ca. 1.5 min.

For all experiments performed the reactor exhaust consisted only of H_2, CO_2, CO, H_2O, O_2 and N_2. The conversion of CO and O_2 and the selectivity of CO were defined as follows:

$$\text{CO conversion}\,(\%) = \frac{[\text{CO}]_{\text{in}} - [\text{CO}]_{\text{out}}}{[\text{CO}]_{\text{in}}} \times 100 \quad (1)$$

$$\text{O}_2\text{ conversion}\,(\%) = \frac{[\text{O}_2]_{\text{in}} - [\text{O}_2]_{\text{out}}}{[\text{O}_2]_{\text{in}}} \times 100 \quad (2)$$

$$\text{CO selectivity}\,(\%) = 0.5 \times \frac{[\text{CO}]_{\text{in}} - [\text{CO}]_{\text{out}}}{[\text{O}_2]_{\text{in}} - [\text{O}_2]_{\text{out}}} \times 100 \quad (3)$$

5. Results and discussion

5.1. CO oxidation activity of catalysts

In the present work, the extent of CO conversion achieved by nine different fresh catalysts in the presence of a dry feed (with excess H_2 and CO_2) is shown in Fig. 5. Five percent Pt/γ-Al_2O_3 was chosen as reference catalyst and was observed to exhibit a conversion of 14% at a temperature of 155 °C. This proved to be the least active catalyst under the present operating conditions as other noble metal catalysts such as 10% Ru/γ-Al_2O_3 and 5% Rh/γ-Al_2O_3 showed conversion levels of 30% and 100% respectively, at a temperature of 155 °C.

A number of reaction paths for CO oxidation have been reported in literature. Kahlich et al. [3] investigated the kinetics of CO over a Pt/Al_2O_3 catalyst in the presence of H_2 and proposed a mechanism similar to that of CO oxidation in the absence of H_2 which justified the decrease in CO conversion at temperatures above 250 °C as being due to a decrease in CO coverage. Nibbelke et al. [23] built their transient kinetic model for CO oxidation in the absence of H_2 over a Pt/Rh/CeO_2/γ-Al_2O_3 catalyst based on three reaction paths. The first was a monofunctional reaction path, which takes into account the competitive adsorption of CO and O_2 on noble metal surface followed by a Langmuir–Hinshelwwod surface reaction. The second was also a monofunctional reaction path which takes into account CO adsorption on an O_2-covered site with subsequent CO_2 desorption. The third path was a bifunctional one where CO is adsorbed onto the noble metal and interacts with the O_2 from ceria present. The present Pt/γ-Al_2O_3, Ru/γ-Al_2O_3, Rh/γ-Al_2O_3 catalysts are thought to engage either of the two monofunctional reaction paths mentioned.

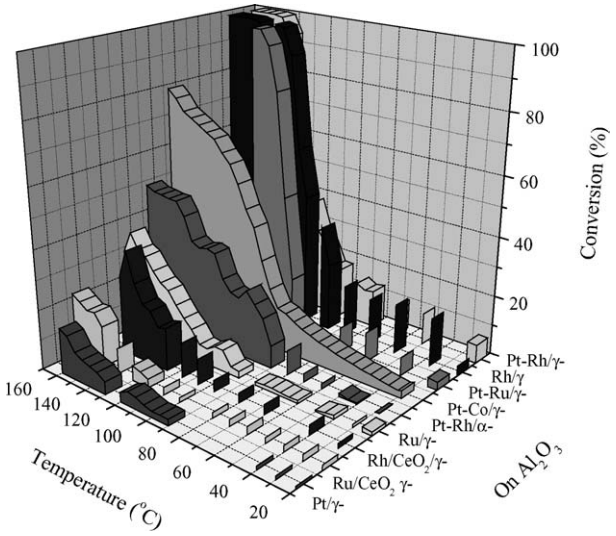

Fig. 5. CO conversion over various catalysts with respect to temperature at a GHSV of 15 500 h^{-1}.

To promote even further the activity of the noble metals, Ru/ceria and Rh/ceria catalysts were prepared onto alumina washcoats so as to achieve CO adsorption onto the noble metal and take advantage of the O_2 storing capabilities of ceria and thus exploit the so-called bifunctional path mentioned previously. The two catalysts, namely 5% Ru/5% CeO_2/γ-Al_2O_3 and 5% Rh/5% CeO_2/γ-Al_2O_3, did display higher activity with respect to Pt/γ-Al_2O_3 yet not with respect to Ru/γ-Al_2O_3 and Rh/γ-Al_2O_3. They achieved 17 and 26% conversions, respectively, at a temperature of 155 °C. The eventual decrease in the activity of Rh/CeO_2/γ-Al_2O_3 could be attributed to the deactivation of the catalyst as the O_2 was not depleted and CO_2 continued to be produced, even though at a lower rate, thus eliminating the possibility of the reverse water–gas-shift reaction taking place. The overall lower activity as compared to the equivalent noble metal on alumina catalysts is considered to be due to the catalyst preparation method. The surface area of the Rh/CeO_2/γ-Al_2O_3 catalyst (given in Table 1) is significantly lower than that of Rh/γ-Al_2O_3 thus affecting activity. The low reduction temperature used may well have been insufficient to promote noble metal ceria interaction but also the presence of high amounts of O_2 may have limited the effect of ceria on overall activity [24,25].

An alternative to the bifunctional path using ceria may be achieved by creating separate active sites for CO and O_2 adsorption through the addition of metal ions such as Ru, Co or Rh. Thus, catalysts with equal loading of Pt and the second noble metal on γ-alumina were prepared and tested. At the temperature of 120 °C, 2.5% Pt–2.5% Ru/γ-Al_2O_3 achieved CO conversion of 45% while 2.5% Pt–2.5% Co/γ-Al_2O_3 and 2.5% Pt–2.5% Rh/γ-Al_2O_3 achieved 95 and 38%, respectively. Pt–Co/γ-Al_2O_3 showed high activity at temperatures up to 120 °C but the rate of

conversion decreased at even higher temperatures implying that temperatures well above the ones investigated would be needed in order to accomplish complete CO oxidation.

Overall, three fresh catalysts achieved 100% conversion (CO below 5 ppm which was the detection limit of the GC) at temperatures up to ca. 150 °C and GHSV of 15 500 h^{-1}. More specifically, 2.5% Pt–2.5% Ru/γ-Al_2O_3 was found to achieve complete CO conversion at a temperature of 126 °C, 5%Rh/γ-Al_2O_3 at 140 °C and 2.5% Pt–2.5% Rh/γ-Al_2O_3 at 143 °C. The operating window for Pt–Ru/γ-Al_2O_3 was up to 130 °C while for the other two catalysts it was at least up to the temperature of 155 °C indicating no significant CO desorption taking place, neither the presence of the reverse water-gas-shift reaction nor of the methanation reaction for all temperatures investigated.

To briefly assess whether the physical properties of the alumina washcoat (such as surface area and presence of hydroxyl groups) play some role, a 2.5% Pt–2.5% Rh/α-Al_2O_3 catalyst was prepared and tested. As is evident from Fig. 5, this catalyst is significantly less active than the equivalent noble metal loading on γ-alumina since at a temperature of 155 °C it achieved 46% conversion as opposed to 100%. In addition, it is less stable as decline in activity is evident at a couple of stages on the graph due to deactivation. On the other hand, the bimetallic nature of the catalyst helps maintain an activity much higher than that of Pt-, Ru-, Ru/CeO_2- and Rh/CeO_2- on γ-alumina.

Even though Pt–Ru/γ-Al_2O_3 was the most active fresh catalyst it also proved to be the least stable. Its limited stability is shown in Fig. 6, where it is evident that after approximately 13 min during the initial experiment, at the temperature of 130 °C, the amount of CO in the off-gas of the reactor began to increase again. The catalyst was allowed to cool down and then the experiment was repeated. Full CO conversion was again achieved by ca. 126 °C as before and when allowed to operate with time at a temperature of 130 °C, CO levels increased once again after 10 min of operation. This time CO concentration levels (2.16%) were well above the inlet concentration (1.12%), while CO_2 levels had reduced at least due to the cease of CO oxidation (to 22%). It can only be assumed that the reverse water-gas-shift (RWGS) reaction was initiated at this point. With time, CO_2 levels built-up while there were possibly only trace amounts of H_2O present thus allowing at a specific temperature the equilibrium of the water–gas-shift reaction to shift towards the reverse direction initiating in this way CO formation. Yan et al. [11] and Kawatsu [26] also observed CO formation due to RWGS but over Pt–Co/Al_2O_3 and Pt/Al_2O_3 catalysts and at temperatures above 160 °C. Within the present study, further work with Pt–Ru/γ-Al_2O_3 catalyst was not pursued due to its unstable nature under the present reaction conditions.

The next most active catalyst, Rh/γ-Al_2O_3, exhibited a much better stability as is shown in Fig. 7. It remained stable for up to 20 h at which point the deactivation became evident as CO levels exceeded 10 ppm and retained an increasing trend for another hour. It was the Pt–Rh/γ-Al_2O_3 catalyst, which after 21.5 h exhibited no evident deactivation. As shown in Fig. 7, the CO level remained below the 5 ppm detection limit of the gas chromatograph. Thus, further experiments were pursued using this type of catalyst.

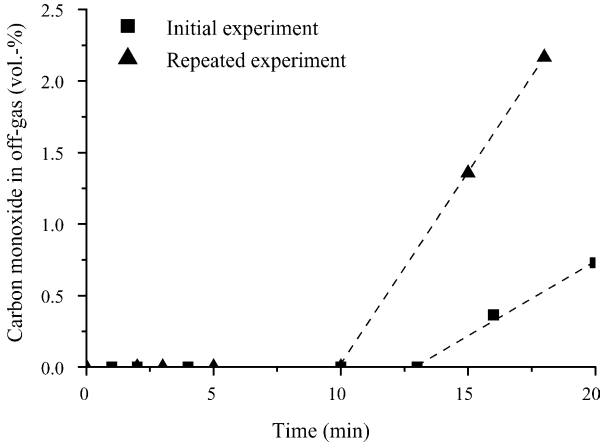

Fig. 6. CO content in off-gas w.r.t. time at 130 °C and GHSV 15 500 h^{-1} over Pt–Ru/γ-Al_2O_3.

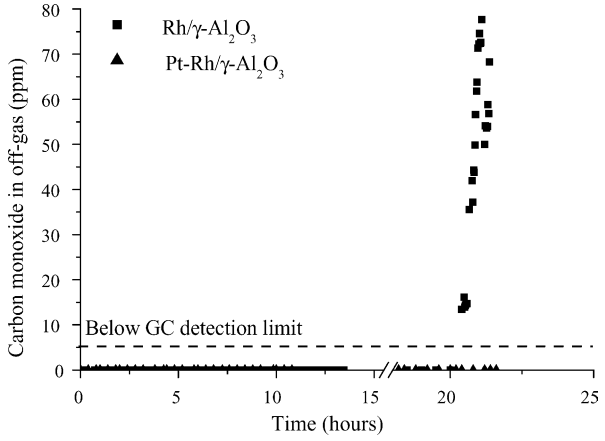

Fig. 7. CO content in off-gas w.r.t. time at GHSV of 15 500 h^{-1} over Rh/γ-Al_2O_3 (at 140 °C) and over Pt–Rh/γ-Al_2O_3 (at 150 °C).

Fig. 8 shows the performance of the 2.5% Pt–2.5% Rh/γ-Al_2O_3 catalyst at a GHSV of 15 500 h^{-1} and using a dry feed. As is evident, with increasing temperature both the CO and O_2 conversion increase. To achieve ca. 100% CO conversion, a

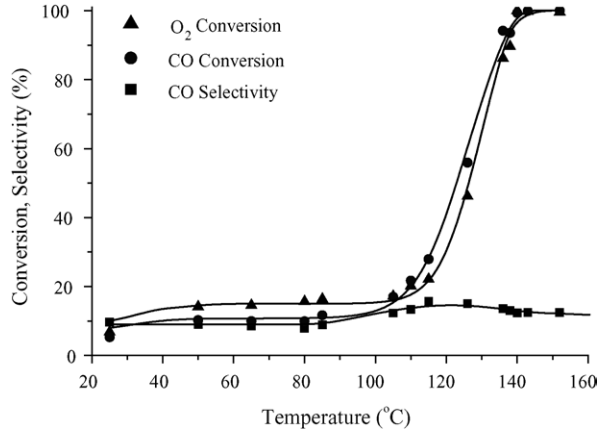

Fig. 8. Temperature effect on CO selectivity and CO and O_2 conversion at GHSV 15 500 h^{-1} over Pt–Rh/γ-Al_2O_3.

temperature of ca. 143 °C was required to be reached at which point almost all of the O_2 was depleted (99.6% conversion). In the low temperature region where CO is expected to cover most of the surface, selectivity increased slowly with temperature and reached a maximum at ca. 120 °C (15%). According to Kahlich et al. [3], even though the H_2 coverage is regarded as being considerably low at low temperatures due to the high CO coverage, a reduction in H_2 coverage takes place with this increase in temperature as H_2 has a lower adsorption energy as CO. Thus, the ratio of the rate of H_2 consumption with respect to rate of CO consumption decreases leading to an increase in CO selectivity. At the point where maximum selectivity is reached CO conversion experiences a sudden increase. From this temperature and onwards CO desorption takes place thus allowing more H_2 to be adsorbed onto the catalyst and subsequently be oxidised to H_2O. Similar behaviour was also observed by Kim and Lim [6] for a Pt/γ-Al_2O_3 catalyst. Selectivity in our case is low (12.5% at 143 °C) due to the high levels of O_2 present in the feed, which are required to bring CO concentration to at least below 50 ppm. The higher amount of O_2 also results in a lower temperature being required for complete CO conversion to be achieved and thus brings operating temperatures to levels applicable for the present fuel processor.

5.2. Effect of O_2/CO ratio

Primary aim of a CO oxidation catalyst for fuel cell applications is to bring CO levels down to at least 50 ppm (if not down to 10 ppm) and maintain stable activity. It is also, though, important to investigate the extent of H_2 loss due to the catalyst selectivity properties at varying O_2/CO ratio. It is known that H_2 oxidation is strongly inhibited by the presence of CO due to the stronger CO chemisorption on the noble metal surfaces as compared to the H_2 and O_2 chemisorption. Consequently, CO covers these active sites allowing few H_2 and O_2 species to weakly chemisorb if temperatures are high enough to desorb some of the CO. Thus, once this stage has been reached, there is simultaneous H_2 and CO oxidation taking place but at different rates.

Fig. 9a is given simply to illustrate that with increasing O_2 amount (the stoichiometric ratio being 0.5) and within the temperature region of 110–115 °C the CO conversion increased relatively linearly for all catalysts. Thus, with all catalysts maximum CO elimination from the reformate stream was achieved with an O_2/CO ratio of 4. Fig. 9b shows the H_2 conversion with varying O_2/CO ratio within the same temperature region. Raising the amount of O_2 inevitably led to an increase in H_2 loss.

Based on Fig. 9a, three sets of catalysts can be identified: the most active (Pt–Ru/γ-Al_2O_3, Rh/γ-Al_2O_3, and Pt–Co/γ-Al_2O_3); those with average activity (Pt–Rh/γ-Al_2O_3, Pt–Rh/α-Al_2O_3, and Rh/CeO_2/γ-Al_2O_3); and the least active (Ru/γ-Al_2O_3, Pt/γ-Al_2O_3 and Ru/CeO_2/γ-Al_2O_3). From the most active catalysts, Pt–Ru/γ-Al_2O_3 showed a pronounced ability to decrease the CO content with increasing O_2 amount. At O_2/CO ratios 1 and 4, the CO conversion was 19 and 64%, respectively.

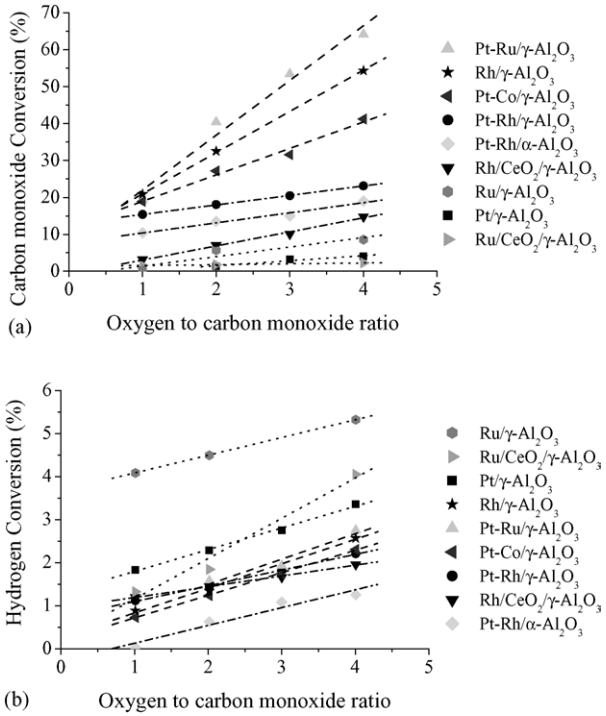

Fig. 9. (a) CO conversion with varying O_2/CO ratio at temperatures between 110 and 115 °C and GHSV 15 500 h^{-1} over various catalysts. (b) H_2 conversion with varying O_2/CO ratio at temperatures between 110 and 115 °C and GHSV 15 500 h^{-1} over various catalysts.

At the same time H_2 conversion reached 2.7% at a ratio of 4; a relatively average loss of H_2 when compared to the other catalysts. This shows that inevitably even though it had a high activity with respect to CO it also exhibited selectivity towards H_2. Rh/γ-Al_2O_3 exhibited the next highest CO conversions. It achieved 24% CO conversion at a ratio of 1 while at a ratio of 4 it achieved 54%. H_2 conversion levels were slightly lower than those of Pt–Ru reaching 2.6% at an O_2/CO ratio of 4. It is also evident that Pt–Co/γ-Al_2O_3 also had a significant effect on CO oxidation, managing to achieve 19% CO conversion at a ratio of 1 and 40% CO conversion at a ratio of 4. H_2 conversion reached the levels of 2.3% at a ratio of 4. Unfortunately these three catalysts have shown in this work to have limitations. As discussed in the previous section, the Pt–Ru/γ-Al_2O_3 prepared did not show stable activity with time while Pt–Co/γ-Al_2O_3 did not succeed in bringing CO levels down to at least 50 ppm at higher temperatures. Rh/γ-Al_2O_3 exhibited good stability for up to 20 h after which deactivation began to be evident.

From the average active catalysts, Pt–Rh/γ-Al_2O_3 showed the highest activity and the highest selectivity. It achieved CO conversion of 15.5% at an O_2/CO ratio of 1 and 23% conversion at a ratio of 4. H_2 conversion reached 2.2% at a ratio of 4. In the previous section, it was shown that this catalysts exhibited stable activity for at least 21.5 h. The next most active catalyst, Pt–Rh/α-Al_2O_3, exhibited the lowest H_2 conversion from all catalysts yet not the lowest CO conversion. The fact that it consumed less hydrogen than all other catalysts may well be due to the lack of OH groups present on its surface, as opposed to the other catalysts, which could assist in the mechanism involved during H_2 conversion. The difference seen in the rate

of H_2 conversion for these three catalysts is considered to be due to the slightly different temperatures in which the measurements were carried out.

The least active catalysts (whose low activity was also evident from the investigations carried out with varying temperature) also exhibited the highest H_2 consumption. This is considered to be mainly due to the insufficient reduction of these catalysts under H_2 during pre-treatment. Thus, regardless of being in the presence of CO these catalysts are found to readily adsorb H_2. The most pronounced H_2 conversion was achieved by the $Ru/CeO_2/\gamma\text{-}Al_2O_3$ catalyst, which also exhibited a higher rate of H_2 conversion with respect to the O_2/CO ratio. Overall though, it is evident that all bimetallic catalysts had higher activity than monometallic catalysts irrespective of surface area properties.

Catalyst pre-treatment is known to be of importance and noble metal catalysts are typically found in literature to be strongly reduced in order to achieve the active metal state. Such treatments though also lead to dehydroxylation of the catalyst thus disabling one reaction path, which is considered to be through the hydroxyl groups. As is shown further on in this contribution, the presence of water (which enables the presence of hydroxyl groups) enhances CO conversion considerable while slightly inhibiting CO selectivity. In addition, under CO oxidation reaction conditions, noble metal catalysts are oxidised leading to further deactivation. Thus, it was judged that for the present work a mild reduction step would be pursued in order to balance catalyst activity with stability.

The most favourable catalyst using the present catalyst preparation method, catalyst pre-treatment and reaction conditions was therefore found to be $Pt–Rh/\gamma\text{-}Al_2O_3$ as it exhibited the best stability with relatively good activity and selectivity. In order to see whether it was active enough to reduce CO down to ppm levels under an O_2/CO ratio of 3 (and thus reduce H_2 loss) its activity was investigated with temperature as shown in Fig. 10. Fifty percent conversion was achieved at a temperature of 135 °C while with a ratio of 4, the same conversion was achieved at 123 °C (see Fig. 8). Thus, the lower amount of O_2 present in the reactant stream inevitably led to the need for a higher temperature in order to achieve similar conversions. The need for higher temperatures though limited the amount of CO conversion obtainable as CO desorption was initiated above 153 °C. Up to this point the activity of the catalyst was high (95.6% conversion reducing CO levels down to 493 ppm) but not high enough for PEM fuel cell operation. Thus, the inlet O_2/CO ratio required for the present $Pt–Rh/\gamma\text{-}Al_2O_3$ catalyst to achieve high levels of CO removal, in a H_2-rich stream and in a single selective oxidation step, was 4. This consequently limited selectivity to the level of 12.5%.

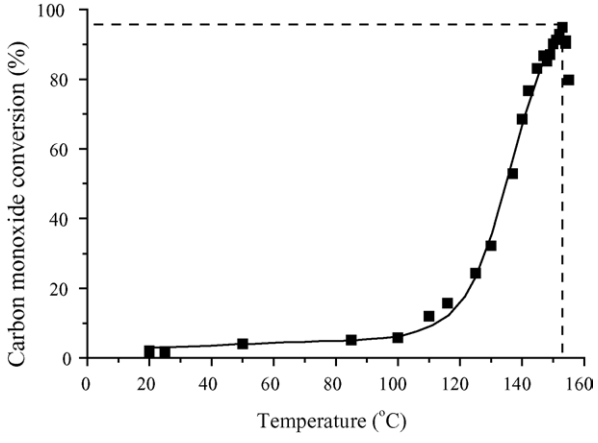

Fig. 10. CO conversion over $Pt–Rh/\gamma\text{-}Al_2O_3$ with varying temperature, O_2/CO ratio of 3 and GHSV 15 500 h^{-1}.

5.3. Effect of H_2O

In order to investigate the effect H_2O has on the activity and selectivity of the $Pt–Rh/\gamma\text{-}Al_2O_3$ catalyst, a wet feed was passed through the reactor while the minimum catalyst temperature was kept above 125 °C so as to ensure that the entire set-up would not have any colder spots which could lead to water condensation and thus flood the reactor and the gas chromatograph.

As shown in Fig. 11a, H_2O had a dramatic effect on CO conversion between the temperatures of 125 and 140 °C. At a temperature of 130 °C, conversion was ca. 68% when no H_2O vapour was present in the feed while it reached 100% when

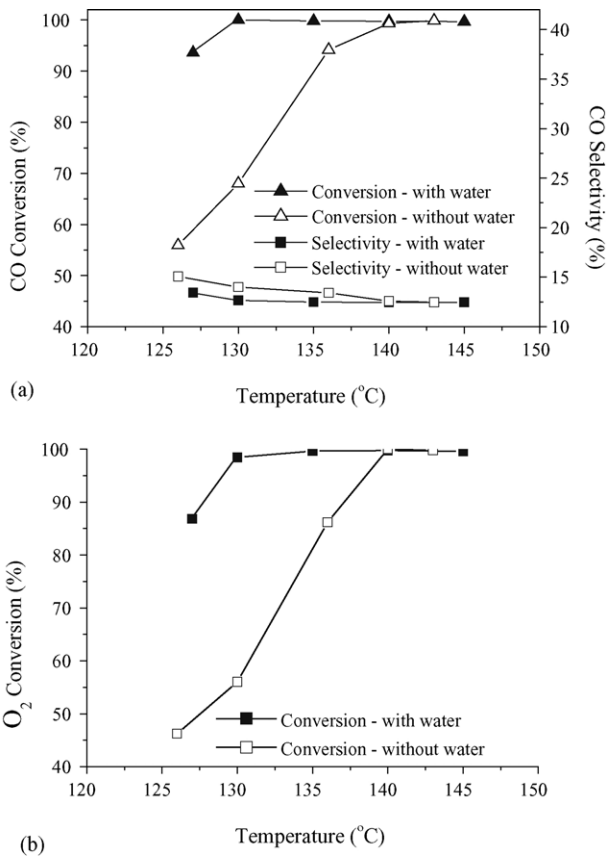

Fig. 11. (a) CO conversion and selectivity over $Pt–Rh/\gamma\text{-}Al_2O_3$ under feeds with and without H_2O, at varying temperatures, O_2/CO inlet ratio of 4 and GHSV of 15 500 h^{-1}. (b) O_2 conversion over $Pt–Rh/\gamma\text{-}Al_2O_3$ under feeds with and without H_2O, at varying temperatures, O_2/CO inlet ratio of 4 and GHSV of 15 500 h^{-1}.

10% H_2O was added. The O_2 consumption (see Fig. 11b) also increased significantly at the temperature of 130 °C achieving 56% when there was no H_2O present and reached ca. 98.5% when there was H_2O present. The influence of H_2O is seen to dominate up to the temperature of ca. 140 °C at which point both CO and O_2 conversions obtained with or without H_2O in the feed reached ca. 100%. The slight drop in CO conversion of about 0.1% experienced between the temperatures of 130 °C until 145 °C during the experiment with the wet feed is attributed to the fact that selectivity dropped due to partial CO desorption thus allowing more H_2 to be converted. Water–gas-shift reaction is not believed to have been present as there was O_2 consumption taking place parallel to CO conversion while there was no H_2 production observed. Fig. 11a also confirms the small influence H_2O has on selectivity. In its presence, selectivity was decreased by maximum 1.5% at a temperature of 130 °C while the effect became insignificant by the temperature of 140 °C. This small influence indicates the increase of both the rate of CO oxidation and the rate of H_2 oxidation in the presence of H_2O (and in effect of OH groups). This is also supported from the fact that as seen in Fig. 11b most of the O_2 was depleted at a 10 °C lower temperature in the presence of H_2O.

The operating window of the catalyst was therefore found to be increased in the presence of H_2O. Similar observations have been made by Manasilp and Gulari [7] who investigated CO oxidation over a Pt/Al_2O_3 catalyst and by Yan et al. [11] who investigated CO oxidation over a $Pt–Co/Al_2O_3$ catalyst. Manasilp and Gulari [7] proposed the possibility that the OH groups formed on the catalyst upon H_2O adsorption are better oxidants than O_2 itself. An interesting mechanism for the influence of OH groups on a Pt/SnOx catalysed CO oxidation reaction has also been suggested by Schryer et al. [27] where modification of the Pt^0 and $Pt(O)_x$ sites takes place. They proposed that OH groups on the surface of a Pt/SnO_2 catalyst (which are regarded as being a significant constituent of tin oxide surfaces) participate in the oxidation of CO chemisorbed on adjacent Pt sites. They observed that pretreatment of catalysts at elevated temperatures partially dehydrates them and thereby significantly depletes the available OH groups. The initial reaction, which occurs when the catalyst is exposed to the test gas mixture further depletes the surface OH groups and partially reoxidises the surface, resulting in an observed catalytic decline. Restoration of surface OH groups by migration of H_2 and/or H_2O from the catalyst bulk eventually restored the catalyst activity [22]. Therefore OH groups used up during the reaction may be replenished by water present in the feed as OH groups are formed by dissociative adsorption of H_2O onto the catalyst. Schubert et al. [28] proposed an interaction taking place between the hydroxylated alumina support and the adsorbed CO leading to the formation of formate species and thus vacating Pt-sites for the adsorption of and dissociation of O_2. This explains the increase in O_2 consumption in a wet feed. A similar mechanism has been proposed by Costello et al. and Kung et al. [29,30] yet where the OH groups are linked to a Au cation.

It is therefore possible that on the present bimetallic catalyst, OH groups are attached onto one of the metal species in addition to being present on the alumina support. The CO may therefore interact with the Rh ion species (as the $Rh/\gamma\text{-}Al_2O_3$ catalyst previously showed higher activity as compared to the $Pt/\gamma\text{-}Al_2O_3$ catalyst indicating CO adsorbs better on Rh than on Pt) thus forming a formate species with the adsorbed OH groups while the O_2 may adsorb onto the Pt species. The adsorbed oxygen then interacts with formate species to form a bicarbonate which subsequently decomposes to CO_2 and which then leaves the catalyst surface.

5.4. Effect of space velocity

As the application of the present selective oxidation catalyst is for a fuel cell system, it is important to determine the effect space velocity has on its performance as it reflects transient operating conditions. As shown in Fig. 12, with higher space velocity the reactant gases (a dry feed was used) had less time over the catalyst to achieve adsorption thus leading to a lower CO conversion at a specific temperature. To achieve 50% CO conversion, a temperature of ca. 140 °C was required to be reached with a space velocity of 31 000 h^{-1} which was ca. 17 °C higher than what was required to achieve the same conversion with a space velocity of 15 500 h^{-1}. At a space velocity of 31 000 h^{-1} and 50% conversion, a CO selectivity of ca. 18% was achieved which was nearly 3% higher than the selectivity achieved at a space velocity of 15 500 h^{-1} and conversion of 50%. This implies that at temperatures above 120 °C and at high space velocities the rate of H_2 conversion decreased with respect to the rate of CO conversion as H_2 adsorption rate was lower than that of CO. CO selectivity though was found at temperatures below ca. 110 °C to be slightly higher at the low space velocity as compared when the space velocity was twice as high thus leading to a higher CO conversion at a specific temperature. This means that at low space velocities and low temperatures (where selectivity increases mildly with temperature) the apparent activation of the H_2 oxidation is lower than that of CO oxidation since the active surface is predominantly covered by adsorbed CO.

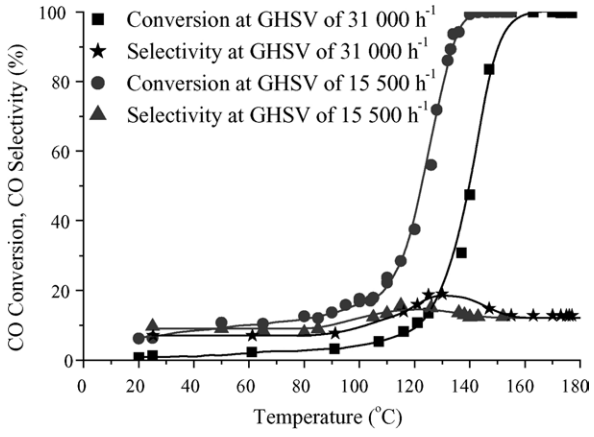

Fig. 12. CO conversion and selectivity over $Pt–Rh/\gamma\text{-}Al_2O_3$ with varying temperature, at O_2/CO inlet ratio of 4 and GHSV of 15 500 and 31 000 h^{-1}.

At temperatures higher than ca. 155 °C, where nearly all of the O_2 had been depleted, selectivity after the optimum peak decreased in both cases to the level of ca. 12.5% which is to be expected with an O_2/CO ratio of 4.

Fig. 13a shows the composition of the off-gas of the reactor with varying catalyst temperature at a GHSV of 15 500 h^{-1} while Fig. 13b shows the composition of the off-gas of the reactor with varying catalyst temperature at a GHSV of 31 000 h^{-1}. It is evident that the rate of H_2O production due to H_2 consumption began to increase at a higher temperature (ca. above 140 °C) when the reactor was run at the higher GHSV of 31 000 h^{-1}. At this space velocity and at temperatures above 110 °C, selectivity with respect to CO was higher thus limiting H_2 consumption. At the respective temperatures, though, where complete CO conversion was achieved in each case, the gas composition of the reactor exit gas was nearly the same. That is, without taking into account the low levels of unreacted O_2 present (<0.01%), in both cases the amount of H_2 was found to lie between 55 and 56%, the amount of CO_2 around 23%, the amount of H_2O around 4–4.5% and the amount of N_2 to lie between 17 and 17.5%. This implies that by doubling the space velocity (and therefore doubling the amount of H_2 flowing through the microstructured reactor) the present selective oxidation microreactor coated with Pt–Rh/γ-Al_2O_3 is capable of converting the CO present in the reformate stream to CO_2 (CO levels are reduced to at least below 50 ppm) by simply running at temperatures above 160 °C and thus allowing a fuel cell to operate with double the power.

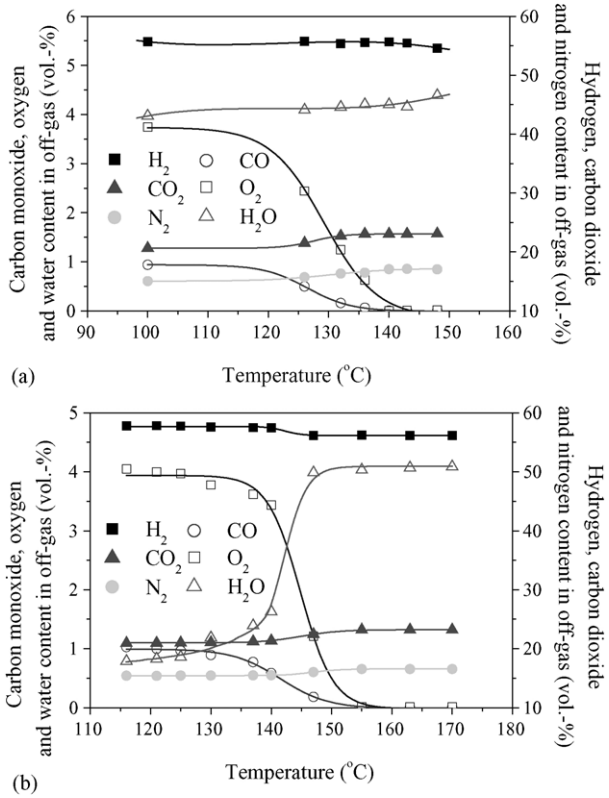

Fig. 13. (a) Off-gas composition with varying temperature, at O_2/CO inlet ratio of 4 and GHSV of 15 500 h^{-1} over Pt–Rh/γ-Al_2O_3. (b) Off-gas composition with varying temperature, at O_2/CO inlet ratio of 4 and GHSV of 31 000 h^{-1} over Pt–Rh/γ-Al_2O_3.

5.5. Effect of catalyst loading and preparation method

The bimetallic catalyst Pt–Rh/γ-Al_2O_3 has been found to be active, relatively selective and stable for CO oxidation under H_2-rich conditions. In order to see if its activity and selectivity can be further improved, instead of preparing it via method A (i.e. mixing a commercial Pt/γ-Al_2O_3 catalyst with a commercial Rh/γ-Al_2O_3 catalyst) it was prepared via method B (i.e. by first preparing a washcoat using a commercial Pt/γ-Al_2O_3 catalyst and then impregnating it with Rh) which also led to an increase in the loading. As shown in Table 1, the catalyst prepared by method B had double the loading and a larger specific surface area (238 m^2/g) than the one prepared by method A (161 m^2/g). The particle sizes were relatively the same yet the values can only be considered qualitatively. As already mentioned, TPR profiles (shown in Fig. 4) indicate that the catalyst prepared by method B had both Pt and Rh species on its surface while the one prepared by method A seems to have had predominantly Rh species on its surface.

To see more clearly the differences in activity and selectivity of the two catalysts, the data are given in tabular form (Table 2). Both the activity and selectivity of the fresh catalyst prepared by method B were much higher at low temperatures (<120 °C) than those of the fresh catalyst prepared by method A. The method B fresh catalyst had a high selectivity of 18.5% at 100 °C while the method A fresh catalyst required a higher temperature in order to exhibit an equivalent selectivity e.g. at 120 °C it reached 15.1%. Thus, the typical maximum of a selectivity peak came later for the method A catalyst indicating that at temperatures below 120 °C O_2 consumption was lower as compared to that of method B catalyst. Fifty percent CO conversion was actually achieved at a temperature of ca. 124 °C by method A fresh catalyst and ca. 109 °C by the method B catalyst. As is evident from Table 2, once

Table 2
CO conversion and selectivity at various temperatures over Pt–Rh/γ-Al_2O_3 catalysts prepared by method A and method B

Temperature (°C)	Method A, fresh Pt–Rh/γ-Al_2O_3		Method B, fresh Pt–Rh/γ-Al_2O_3		Method B, aged Pt–Rh/γ-Al_2O_3[a]	
	X_{CO} (%)	S_{CO} (%)	X_{CO} (%)	S_{CO} (%)	X_{CO} (%)	S_{CO} (%)
80	9.9	8.3	20.7	16.5	11.8	28.7
100	14.5	10.6	35.3	18.5	24.7	22.4
120	34.6	15.1	83.2	14.5	76.2	12.4
140	99.4	12.4	99.8	12.4	99.9	12.5
145	99.9	12.4	99.9	12.4	99.9	12.5

[a] After 50 h.

very high CO conversion levels were achieved by both catalysts (>99%) selectivity was the same for both (ca. 12.5%) as O_2 depletion had reached for both cases very high levels (>99%) making it the limiting factor. Thus, the loss of H_2 was the same for both catalysts at temperatures where CO conversion was well above 90%.

The performance of method B catalyst was further investigated. More specifically, its activity and selectivity were tested again after 50 h of operation in the temperature region of 138–158 °C (aged method B catalyst in Table 2). It can be seen that selectivity at low temperatures improved further implying that the catalyst surface was modified after 50 h of operation. Conversion levels were found to have decreased for temperatures at least below 140 °C but nevertheless, 99.9% CO conversion was still achieved above 140 °C.

High conversion and selectivity at low temperatures is of importance during start-up and varying load conditions as high CO conversion levels and low H_2 loss is also desired. The fact that method B catalyst was more selective at low temperatures as compared to method A catalyst may not only be due to the higher loading but also due to the fact that the Pt and Rh species achieve better synergy due to better dispersion of both active species on the catalyst surface (and thus higher surface area). As previously suggested, CO may preferably adsorb onto the Rh species thus allowing Pt free sites for O_2 adsorption. OH groups are present on the support and may also interact with a metal cation. They are expected to play more of a role at low temperatures than high temperatures with dry feeds yet throughout the temperature range during operation with wet feeds (which was not the case here). Confirming the actual reaction pathway was beyond the scope of the present work.

To improve catalyst performance further, it is suggested that in the future catalysts should be calcined at a lower temperature of ca. 400 °C in order to achieve higher dispersion and the pre-treatment under H_2 should be carried out at the slightly higher temperature of 150 °C. Co-precipitation is also currently pursued as a catalyst preparation method in our group in order to achieve better dispersion and small particle sizes of the active species.

5.6. Catalyst long term operation

Prior to the long term testing of the Pt–Rh/γ-Al_2O_3 catalyst prepared by method B under dry feed conditions, the catalyst was heated up from room temperature to 155 °C in 2 h where the CO content decreased significantly from 1.12%. As can be seen in Fig. 14a, with increasing temperature the levels of CO decreased down to 5 ppm until ca. 155 °C was reached. At this point the levels increased again to just above 30 ppm indicating that the catalyst possibly needs some time in order to achieve stable activity. From this point onwards, data were collected while the reactor was operated for 50 h while temperatures were varied between 138 and 158 °C as shown in Fig 14b. During approximately the first 5 h after having reached 155 °C, a slight activation of the catalyst took place as the amount of CO was reduced from ca. 30 ppm to ca. 26 ppm at a constant temperature. The catalyst was allowed to run under these conditions for

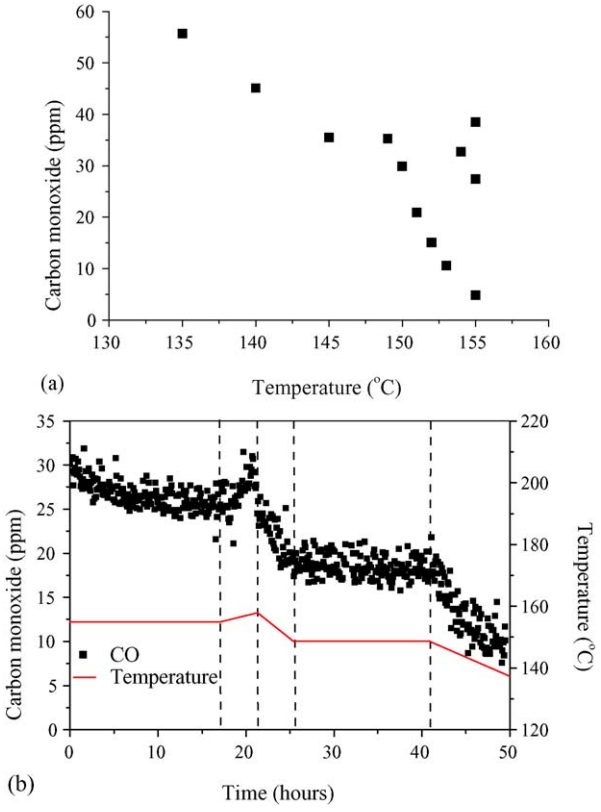

Fig. 14. (a) Pt–Rh/γ-Al_2O_3 catalyst operation with varying temperature, O_2/CO inlet ratio of 4 and GHSV of 15 500 h^{-1}. (b) Pt–Rh/γ-Al_2O_3 catalyst operation with time, at O_2/CO inlet ratio of 4 and GHSV of 15 500 h^{-1}.

approximately another 12 h as it was judged that the detection of CO gave a better picture of the catalyst stability as opposed to no detection at all. The catalyst exhibited stable activity during this period. In pursuit of decreasing the CO content even further, the catalyst temperature was gradually increased to 158 °C during 4 h. It was noticed though that the CO amount increased again to ca. 30 ppm. The temperature was therefore decreased to 149 °C during another 4 h. The CO content decreased down to ca. 18 ppm. The catalyst was left for ca. 25 h to operate under these conditions and it again exhibited stable behaviour throughout. The fact that conversion increased in a stable manner with decreasing temperature leads to the conclusion that CO desorption was encouraged at high temperatures. After 40 h of total operation, the catalyst temperature was decreased further to 138 °C during a 10 h period. The average concentration of CO reached at this temperature was ca. 12 ppm while the lowest was 7 ppm once this temperature was reached.

The catalyst therefore proved to have stable behaviour for 50 h in addition to exhibiting a broad operating temperature window; that is at least between 138 and 158 °C the CO content was between 10 and 30 ppm which is important when considering fluctuations typically experienced during operation of entire fuel processors.

Literature on good long term performance of selective oxidation reactors achieving CO conversions below 30 ppm is limited. Chen et al. [16] operated a microstructured reactor coated with a Rh–K/Al_2O_3 catalyst at GHSV of 20 000 h^{-1}, and temperature of ca. 190 °C and O_2/CO ratio of 1.5 for 60 h which

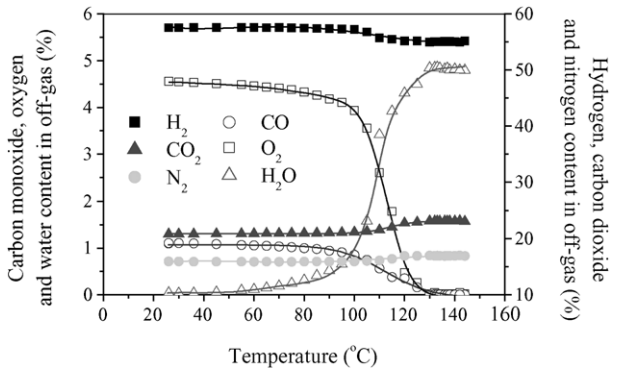

Fig. 15. Off-gas composition with varying temperature, at O_2/CO inlet ratio of 4 and GHSV of 15 500 h^{-1} over aged Pt–Rh/γ-Al_2O_3 prepared by method B.

converted 0.5% CO in a H_2-rich stream to 20 ppm. Dudfield et al. [17] operated a compact reactor for 3 h using a Pt–Ru/hopcalite catalyst which reduced 0.7% CO to below 20 ppm at a temperature of ca. 150 °C and O_2/CO ratio of 3. By passing the reformate stream through two selective oxidation reactors they achieved reduction of 0.5% CO to 10–20 ppm for 40 h. Dudfield et al. [15] further published results from the operation in series of two selective oxidation reactors for 3 h showing reduction of 1.6% CO to below 10 ppm.

5.7. Power output of device

The power output of the microstructured reactor used in the present work was assessed based on its operation when coated with the method B Pt–Rh/γ-Al_2O_3 catalyst. Fig. 15 shows the off-gas composition with varying temperature at O_2/CO inlet ratio of 4 and GHSV of 15 500 h^{-1} over the aged catalyst. Under these conditions, a clean H_2 stream (with less than 10 ppm CO present), which could power a 28 W PEM fuel cell (assuming 64% fuel cell efficiency and 80% H_2 utilisation) was delivered by this reactor. Based on results presented earlier in the paper, with double the reformate stream flowrate (i.e. GHSV of 31 000 h^{-1}) the catalyst can achieve CO clean-up by simply increasing the temperature by another 17 °C. Thus, under these conditions the power output of the device would be double.

In general, CO conversion achieved is high; selectivity though is limited by the high oxygen amount present. With the present catalyst, the only way to reduce H_2 loss (and thus increase power output) is to carry out CO clean-up in two stages. In this way, the total amount of air given at the first stage is minimised as much as possible (there is of course a limit) and the CO oxidation is completed at the second stage usually with less air present as compared to the first stage. In this way CO surface coverage as a function of temperature is more controlled leading to less free sites being available for H_2 oxidation. Dual-stage systems have been used in other fuel processors for this very reason [15,31]. The disadvantage of this solution is that the number of devices present in a fuel processor is higher thus making it less compact and its control more complex leading to even higher costs. Thus, the importance of minimising H_2 loss needs to be judged with regards to overall system efficiency, size, complexity and costs.

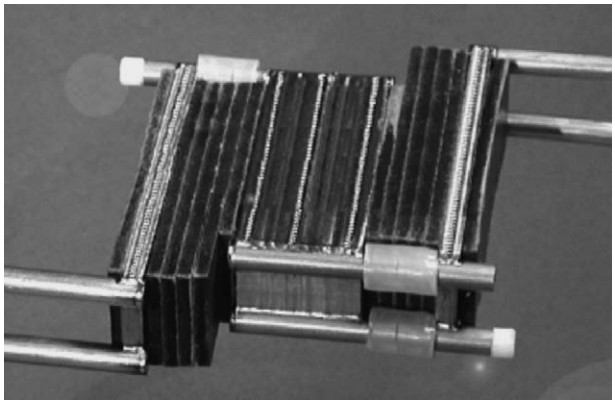

Fig. 16. Improved selective oxidation-heat exchanger microstructured reactor.

To improve the power density, heat exchange performance and consequently start-up time of the reactor developed within the MiRTH-e project, an improved version has been built (shown in Fig. 16). It is significantly more compact (external dimensions of 17 mm × 64 mm × 55 mm) while it is a welded structure. The performance of this device and suitability of reactor design has been reported by Delsman et al. [21].

6. Conclusion

The Pt–Rh/γ-Al_2O_3 catalyst was found to be active under CO oxidation conditions in the presence of excess H_2, CO_2 and H_2O and within the temperature range defined by the fuel processing unit (140–160 °C). It exhibited stable activity in a dry feed for at least 50 h and succeeded in bringing CO concentration down to ca. 10 ppm from an inlet concentration of 1.12%, which is desired for efficient PEM fuel cell operation. The presence of water in the reactant feed was found to promote catalyst activity possibly due to the involvement of adsorbed OH groups in the reaction path.

Improved selectivity (and thus reduced H_2 loss) while achieving CO reduction from ca. 1% to 10 ppm over the present catalyst can only be achieved in a dual-stage reactor system. In this way the O_2/CO ratio may be reduced without affecting conversion levels.

Acknowledgements

The authors gratefully acknowledge funding from the European Commission for the project ‘Micro Reactor Technology for Hydrogen and Electricity’ (MiRTH-e), contract number ENK6-CT-2000-00110, under the ‘Energy, Environment and Sustainable Development’ Programme. Porotec GmbH is also acknowledged for providing the TPR measurements.

References

[1] A.F. Ghenciu, Curr. Opin. Sol. St. Mater. Sci. 6 (2002) 389.
[2] G. Avgouropoulos, T. Ioannides, Ch. Papadopoulou, J. Batista, S. Hocevar, H. Matralis, Catal. Today 75 (2002) 157.
[3] M.J. Kahlich, H.A. Gasteiger, R. Behm, J. Catal. 171 (1997) 93.

[4] M.M. Schubert, M.J. Kahlich, H.A. Gasteiger, R.J. Behm, J. Power Sources 84 (1999) 175.
[5] A. Eichler, Surf. Sci. 498 (2002) 314.
[6] D.H. Kim, M.S. Lim, Appl. Catal. A 224 (2002) 27.
[7] A. Manasilp, E. Gulari, App. Catal. B 37 (2002) 17.
[8] I.H. Son, A.M. Lane, D.T. Johnson, J. Power Sources 124 (2003) 415.
[9] O. Korotkikh, R. Farrauto, Catal. Today 62 (2000) 249.
[10] X. Liu, O. Korotkikh, R. Farrauto, Appl. Catal. A 226 (2002) 293.
[11] J. Yan, J. Ma, P. Cao, P. Li, Catal. Lett. 93 (2004) 55.
[12] S.H. Oh, R.M. Sinkevitch, J. Catal. 142 (1993) 254.
[13] P.V. Snytnikov, V.A. Sobyanin, V.D. Belyaev, P.G. Tsyrulnikov, N.B. Shitova, D.A. Shlyapin, Appl. Catal. A 239 (2003) 149.
[14] D.L. Trimm, Z.I. Önsan, Catal. Rev. 43 (2001) 31.
[15] C.D. Dudfield, R. Chen, P.L. Adcock, Int. J. Hydrogen Energy 26 (2001) 763.
[16] G. Chen, Q. Yuan, H. Li, S. Li, Chem. Eng. J. 101 (2004) 101.
[17] C.D. Dudfield, R. Chen, P.L. Adcock, J. Power Sources 85 (2000) 237.
[18] C.D. Dudfield, R. Chen, P.L. Adcock, J. Power Sources 86 (2000) 214.
[19] G. Kolb, V. Hessel, Chem. Eng. J. 98 (2004) 1.
[20] E.R. Delsman, M.H.J.M. de Croon, G.J. Kramer, P.D. Cobden, C. Hofmann, V. Cominos, J.C. Schouten, Chem. Eng. J. 101 (2004) 123.
[21] E.R. Delsman, M.H.J.M. de Croon, A. Pierik, G.J. Kramer, P.D. Cobden, C. Hofmann, V. Cominos, J.C. Schouten, Chem. Eng. Sci. 59 (2004) 4795.
[22] D.R. Schryer, B.T. Upchurch, J.D. Van Norman, K.G. Brown, J. Schryer, J. Catal. 122 (1990) 193.
[23] R.H. Nibbelke, A.J.L. Nievergeld, J.H.B.J. Hoebink, G.B. Marin, Appl. Catal. B 19 (1998) 245.
[24] S. Özkara, A.E. Aksoylu, Appl. Catal. A 251 (2003) 75.
[25] I.H. Son, A.M. Lane, Catal. Lett. 76 (2001) 151.
[26] S. Kawatsu, J. Power Sources 71 (1998) 150.
[27] D.R. Schryer, B.T. Upchurch, B.D. Sidney, K.G. Brown, G.B. Hoflund, R.K. Herz, J. Catal. 130 (1991) 314.
[28] M.M. Schubert, H.A. Gasteiger, R.J. Behm, J. Catal. 172 (1997) 256.
[29] C.K. Costello, M.C. Kung, H.-S. Oh, Y. Wang, H.H. Kung, Appl. Catal. A 232 (2002) 159.
[30] H.H. Kung, M.C. Kung, C.K. Costello, J. Catal. 216 (2003) 425.
[31] S.H. Lee, J. Han, K.Y. Lee, J. Power Sources 109 (2002) 394.